

Shock breakout driven by the remnant of a neutron star binary merger: An X-ray precursor of mergernova emission

Shao-Ze Li and Yun-Wei Yu

ABSTRACT

A supra-massive neutron star (NS) spinning extremely rapidly could survive from a merger of NS-NS binary. The spin-down of this remnant NS that is highly magnetized would power the isotropic merger ejecta to produce a bright mergernova emission in ultraviolet/optical bands. Before the mergernova, the early interaction between the NS wind and the ejecta can drive a forward shock to propagate outwards into the ejecta. As a result, a remarkable amount of heat can be accumulated to be deposited behind the shock front, the final escaping of which can produce a shock breakout emission. We describe the dynamics and thermal emission of this shock with a semi-analytical model. It is found that a sharp and luminous breakout emission, which is mainly in soft X-rays with a luminosity of $\sim 10^{45}$ erg s $^{-1}$, appears at a few hours after the merger, by leading the mergernova emission as a precursor. Therefore, detections of such X-ray precursors would provide a smoking-gun evidence for identifying NS-powered mergernovae and distinguishing them from the radioactive-powered ones (i.e., kilonovae or macronovae). The discovery of NS-powered mergernovae would finally help to confirm the gravitational wave signals due to the mergers and the existence of supra-massive NSs.

Subject headings: gamma-ray burst: general — stars: neutron — supernovae: general

1. Introduction

A merger of binary neutron stars (NSs) is one of the most promising targets of direct detection of gravitational waves (GWs). It is expected that, in the very near future, the second generation of ground-based GW detectors would extend the detection horizons of the

¹Institute of Astrophysics, Central China Normal University, Wuhan 430079, China, yuyw@mail.cnu.edu.cn

mergers to a few hundred Mpc (Abadie et al. 2010; Nissanke et al. 2013). For achieving such an expectation, some observations of electromagnetic counterparts of the GW signals are necessarily needed, which can help to confirm the position, time, redshift, and astrophysical properties of the GW sources.

During a NS-NS merger event, the rapidly rotating compact system could eject a highly collimated relativistic jet and a quasi-isotropic sub-relativistic outflow, where various electromagnetic emission could be produced. Specifically, internal and external dissipations of the jet energy can result in a short-duration gamma-ray burst (GRB) and its multi-wavelength afterglow emission, respectively, which could be the most attractive electromagnetic counterparts in view of their high brightness (see Nakar 2007, Berger 2014 for reviews). However, unfortunately, the detection probability of an associated GRB is significantly suppressed by the small opening angle of the jet (Fong et al. 2014), although a late and weak orphan afterglow could still be observed by off-axis (van Eerten & MacFadyen 2011; Metzger & Berger 2012). Alternatively, more and more attentions have been paid to the emission originated from the isotropic ejecta, e.g., thermal emission due to the diffusion of internal energy of the ejecta (called mergernova by Yu et al. 2013; Li & Paczynski 1998; Kulkarni 2005; Rosswog 2005; Metzger et al. 2010) and non-thermal emission due to the shock interaction between the ejecta and environment medium (Nakar & Piran 2011; Metzger & Berger 2012; Piran et al. 2013; Gao et al. 2013).

The isotropic merger ejecta is probably highly neutron-rich, which makes it possible to effectively synthesize nuclei much heavier than ^{56}Ni via rapid neutron capture processes (r-processes; Rosswog et al. 1999, 2014; Roberts et al. 2011; Goriely et al. 2011; Korobkin et al. 2012; Bauswein et al. 2013a; Hotokezaka et al. 2013, 2015; Wanajo et al. 2014; Goriely 2015; Just et al. 2015; Martin et al. 2015). The radioactive decays of these newly synthesized elements can heat the ejecta to produce a detectable thermal emission. Nevertheless, being limited by the element synthesis efficiency and the low mass of the ejecta (no more than a few percent of solar mass), the luminosity of a radioactive-powered mergernova is expected to be not much higher than $\sim 10^{41}\text{erg s}^{-1}$. Thus these phenomena are widely known as kolinova or macronova (Kulkarni 2005; Metzger et al. 2010; Barnes & Kasen 2013; Tanaka & Hotokezaka 2013; Grossman et al. 2014; Kasen et al. 2015).

Such a luminosity limit can be exceeded if a more powerful energy source can be provided by the central post-merger compact object. By invoking a remnant supra-massive NS that spins extremely rapidly and is highly magnetized, Yu et al. (2013) and Metzger & Piro (2014) had investigated the mergernova emission powered by the spin-down energy of the NS. It was found that the peak luminosity of such a NS-powered mergernova, which of course depends on the lifetime of the NS and the collimation of the NS wind, could sometimes be comparable

to and even exceed the luminosity of ordinary supernovae, but with a much shorter duration on the order of a few days. In the aspect of observation, some unusual rapidly evolving and luminous transients were discovered by the Pan-STARRS1 Medium Deep Survey (Drout et al. 2014). The characteristics of these transients are basically consistent with the predictions for NS-powered mergernovae (Yu et al. 2015), although multi-wavelength cross-identifications are still demanded.

Recently some multi-wavelength studies have already been carried out on observational candidates of mergernovae. For example, being indicated by the shallow-decay afterglows of GRB 130603B, the widely-discussed infrared excess after this GRB is probably powered by a remnant NS (Fan et al. 2013) rather than by radioactivities as usually considered (Tanvir et al. 2013; Berger et al. 2013). More directly, by considering of the high-energy emission from a NS wind (Yu et al. 2010; Zhang 2013), which can partly leak from a preceding merger ejecta at late time, a NS-powered mergernova is expected to be possibly accompanied by a late X-ray re-brightening. Very recently Gao et al. (2015) found that the late optical and X-ray bumps after GRB 080503 provided a perfect sample for such a multi-wavelength feature. In this paper, going ahead, we would reveal another possible X-ray signature prior to a NS-powered mergernova, which is caused by the breakout of the shock arising from the early interaction between the NS wind and the merger ejecta. This X-ray precursor emission would play an essential role in future mergernova identifications and in GW detections.

2. The model

2.1. Remnant neutron star and merger ejecta

A merger would happen inevitably in a NS-NS binary when the gravity between the NSs can no longer be supported by angular momentum because of GW radiation release. After the merger, in some situations, a supra-massive NS rather than a black hole could be left with an extremely rapid differential rotation, which is supported indirectly by many emission features of short GRBs and afterglows including extended gamma-ray emission, X-ray flares, and plateaus (Dai et al. 2006; Fan & Xu 2006; Zhang 2013; Giacomazzo & Perna 2013; Rowlinson et al. 2010, 2013). The presence of such a supra-massive NS is permitted by both theoretical simulations (Bauswein et al. 2013b; Hotokezaka et al. 2011) and observational constraints (e.g., the present lower limit of the maximum mass of Galactic NSs is precisely set by PSR J0348+0432 to $2.01 \pm 0.04 M_{\odot}$; Antoniadis et al. 2013). During the first few seconds after the birth of a remnant NS, on one hand, a great amount of neutrinos can be emitted from the very hot NS. On the other hand, differential rotation of the NS can generate multipolar magnetic fields through some dynamo mechanisms (Duncan & Thompson 1992;

Price & Rosswog 2006; Cheng & Yu 2014), making the NS to be a magnetar. Consequently, during the very early stage, the neutrino emission and ultra-strong magnetic fields together could drive a continuous baryon outflow (Dessart et al. 2009; Siegel et al. 2014; Siegel & Ciolfi 2015), which contributes an important component to an isotropic merger ejecta. A few of seconds later, the NS eventually enters into an uniform rotation stage and meanwhile a stable dipole structure of magnetic fields can form. From then on, the NS starts to lose its rotational energy via a Poynting flux-dominated wind. The spin-down luminosity carried by the wind can be estimated with the magnetic dipole radiation formula as $L_{\text{sd}} = L_{\text{sd},i} (1 + t/t_{\text{md}})^{-2}$, where $L_{\text{sd},i} = 10^{47} \mathcal{R}_{s,6}^6 \mathcal{B}_{14}^2 \mathcal{P}_{i,-3}^{-4} \text{ erg s}^{-1}$, $t_{\text{md}} = 2 \times 10^5 \mathcal{R}_{s,6}^{-6} \mathcal{B}_{14}^{-2} \mathcal{P}_{i,-3}^2 \text{ s}$, and the zero point of time t is set at the beginning of the magnetic dipole radiation which is somewhat later than the NS formation by several seconds. Here \mathcal{R}_s , \mathcal{B} , and \mathcal{P}_i are the radius, dipolar magnetic field strength, and initial spin periods of the NS, respectively, and the convention $Q_x = Q/10^x$ is adopted in cgs units.

During a merger event, although the overwhelmingly majority of matter finally falls into the central remnant NS, there is still a small fraction of matter ejected outwards, e.g., the baryon wind blown from the NS mentioned above. Besides that component, an quasi-isotropic merger ejecta can also be contributed by a wind from a short-lived disk surrounding the NS, by an outflow from the colliding interface between the two progenitor NSs, and by a tidal tail due to the gravitational and hydrodynamical interactions. The latter two components are usually called dynamical components. These ejecta components differ with each other in masses, electron fractions, and entropies. It is difficult and nearly impossible to precisely describe the specific constituents and distributions of a merger ejecta, which depend on the relative sizes of the two progenitor NSs, equation of states of NS matter, and magnetic field structures. In any case, according to the numerical simulations in literature, on one hand, the mass of dynamical components could range from $\sim 10^{-4} M_\odot$ to a few times $\sim 0.01 M_\odot$ (Oechslin et al. 2007; Bauswein et al. 2013a; Hotokezaka et al. 2013; Rosswog 2013). On the other hand, in presence of a remnant supra-massive NS, the mass of a neutrino-driven wind is found to be at least higher than $3.5 \times 10^{-3} M_\odot$ (Perego et al. 2014), and the mass-loss rate due to ultrahigh magnetic fields is about $10^{-3} - 10^{-2} M_\odot \text{ s}^{-1}$ during the first 1 – 10 s (Siegel et al. 2014). Therefore, by combining all of these contributions (see Rosswog 2015 for a brief review), we would take $M_{\text{ej}} = 0.01 M_\odot$ as a reference value for the total mass of an ejecta. Furthermore, we would adopt power-law density and velocity distributions of this mass as follows (Nagakura et al. 2014):

$$\rho_{\text{ej}}(r, t) = \frac{(\delta - 3) M_{\text{ej}}}{4\pi r_{\text{max}}^3} \left[\left(\frac{r_{\text{min}}}{r_{\text{max}}} \right)^{3-\delta} - 1 \right]^{-1} \left(\frac{r}{r_{\text{max}}} \right)^{-\delta}, \quad (1)$$

and

$$v_{\text{ej}}(r, t) = v_{\text{max}} \frac{r}{r_{\text{max}}(t)}, \quad \text{for } r \leq r_{\text{max}}(t), \quad (2)$$

where r is the radius to the central NS, v_{max} is the maximum velocity of the head of ejecta which is probably on the order of $\sim 0.1c$, and the slope δ ranges from 3 to 4 according to the numerical simulation of Hotokezaka et al. (2013). In this paper we take $\delta = 3.5$ as in Nagakura et al. (2014). The maximum radius of ejecta can be calculated by $r_{\text{max}}(t) \approx r_{\text{max},i} + v_{\text{max}}t$, where $r_{\text{max},i} \approx v_{\text{max}}\Delta t$ with Δt being the time on which the dipolar magnetic field is stabilized. Correspondingly, the minimum radius reads $r_{\text{min}}(t) = r_{\text{min},i} + v_{\text{min}}t$ and its initial value could be determined by an escape radius as $r_{\text{min},i} = (2GM_c r_{\text{max},i}^2 / v_{\text{max}}^2)^{1/3}$, where G is the gravitational constant and M_c is the mass of the remnant NS.

2.2. Shock heating and emission

The huge energy released from the spin-down of a millisecond magnetar would eventually drive an ultra-relativistic wind mixing Poynting flux and leptonic plasma. Some internal dissipations (e.g. the ICMART processes; Zhang & Yan 2011) in such a leptonic wind could produce non-thermal high-energy emission. Meanwhile, a termination shock could be formed when the wind collides with the preceding merger ejecta, if the wind magnetization has become sufficiently low (Dai 2004; Mao et al. 2010; Wang et al. 2015). In any case, the material at the bottom of merger ejecta would be firstly heated by receiving heat from the termination-shocked region and by absorbing high-energy photons from the deeper wind. Then the high internal pressure of the ejecta material at the bottom can lead itself to expand adiabatically and to reach a high speed. This speed would result in the formation of a forward shock which further catches up with ejecta materials at much larger radii. The increase rate of the mass of shocked ejecta reads

$$\frac{dM}{dt} = 4\pi r_{\text{sh}}^2 [v_{\text{sh}} - v_{\text{ej}}(r_{\text{sh}}, t)] \rho_{\text{ej}}(r_{\text{sh}}, t), \quad (3)$$

where r_{sh} is the radius of shock front, v_{sh} is the shock speed, $v_{\text{ej}}(r_{\text{sh}}, t)$ and $\rho_{\text{ej}}(r_{\text{sh}}, t)$ are the velocity and density of the upstream material just in front of the shock. Obviously, we also have $dr_{\text{sh}} = v_{\text{sh}}dt$.

As the propagation of a shock, its bulk kinetic energy, which is previously gained from adiabatic acceleration, can again be partly converted into the internal energy of newly shocked material. The rate of this shock heating effect can be calculated by

$$H_{\text{sh}} = \frac{1}{2} [v_{\text{sh}} - v_{\text{ej}}(r_{\text{sh}}, t)]^2 \frac{dM}{dt}. \quad (4)$$

Then the total internal energy accumulated by the shock can be derived from

$$\frac{dU_{\text{sh}}}{dt} = H_{\text{sh}} - P_{\text{sh}} \frac{d(\epsilon V)}{dt} - L_{\text{sh}}, \quad (5)$$

where $P_{\text{sh}} = U_{\text{sh}}/(3\epsilon V)$ is the pressure, $V \sim (4/3)\pi r_{\text{sh}}^3$ is the volume of the whole shocked region experiencing an adiabatic expansion, the fraction ϵ is introduced by considering that the shock-accumulated heat is mostly deposited at a small volume immediately behind the shock front, and L_{sh} is the luminosity of shock thermal emission due to the diffusion of shock heat into the unshocked ejecta and eventually escape from the outmost surface of merger ejecta.

By approximately following a steady diffusion equation $L = (4\pi r^2/3\kappa\rho)(\partial u/\partial r)$, where κ is opacity, ρ and u are densities of mass and internal energy, respectively, we roughly estimate the luminosity of shock thermal emission by

$$L_{\text{sh}} \approx \frac{r_{\text{m}}^2 U_{\text{sh}} c}{\epsilon r_{\text{sh}}^3 + (r_{\text{m}}^3 - r_{\text{sh}}^3)} \left[\frac{1 - e^{-(\epsilon\tau_{\text{sh}} + \tau_{\text{un}})}}{\epsilon\tau_{\text{sh}} + \tau_{\text{un}}} \right], \quad (6)$$

where $\tau_{\text{sh}} = \kappa M_{\text{sh}}/4\pi r_{\text{sh}}^2$ and $\tau_{\text{un}} = \int_{r_{\text{sh}}}^{r_{\text{max}}} \kappa \rho_{\text{ej}} dr$ are the optical depths of the shocked and unshocked ejecta, respectively. Here the former optical depth, which only influences the decrease of the shock emission after breakout, is calculated by considering that the most of shocked material is concentrated within a thin shell behind the shock front. The value of parameter ϵ can be fixed by equating the shock luminosity during breakout to the simultaneous heating rate, because after that moment the freshly-injected shock heat can escape from the ejecta nearly freely. The opacity of merger ejecta is predicted to be on the order of magnitude of $\sim (10 - 100) \text{ cm}^2 \text{ g}^{-1}$, which results from the bound-bound, bound-free, and free-free transitions of lanthanides synthesized in the ejecta (Kasen et al. 2013). This value is much higher than the typical one of $\kappa = 0.2 \text{ cm}^2 \text{ g}^{-1}$ for normal supernova ejecta. In this paper we take $\kappa = 10 \text{ cm}^2 \text{ g}^{-1}$. Fairly speaking, some reducing effects on the opacity could exist, e.g., (1) the lanthanide synthesis in the wind components of ejecta could be blocked by neutrino irradiation from the remnant NS by enhancing electron fractions (Metzger & Fernández 2014) and (2) the lanthanides in the dynamical components could be ionized by the X-ray emission from the NS wind (Metzger & Piro 2014).

2.3. Shock dynamics

The temporal evolution of shock thermal emission, as presented in Equation (6), is obviously dependent on the dynamical evolution of the shock, which can be derived from the

energy conservation law. The total energy of shocked region, can be written as¹ $E = \frac{1}{2}Mv_{\text{sh}}^2 + U$, where U is the total internal energy of the shocked region which is much larger than U_{sh} . In principle, the concept “shocked region” used here can also include the termination shock region of NS wind, if it exists, because both the forward shock and wind termination shock are radiation-dominated and the mass of wind leptons is drastically smaller than that of shocked ejecta. By ignoring the relatively weak energy supply by radioactivities, the variation of the total energy can be written as

$$dE = (\xi L_{\text{sd}} - L_e)dt + \frac{1}{2}v_{\text{ej}}^2(r_{\text{sh}}, t)dM, \quad (7)$$

where ξ represents the energy injection efficiency from the NS wind, which could be smaller than one if the NS wind is highly anisotropic, and L_e is the total luminosity of the thermal emission of merger ejecta. Substituting the expression of E into Equation (7), we can get the dynamical equation of the forward shock as

$$\frac{dv_{\text{sh}}}{dt} = \frac{1}{Mv_{\text{sh}}} \left[(\xi L_{\text{sd}} - L_e) - \frac{1}{2}(v_{\text{sh}}^2 - v_{\text{ej}}^2) \frac{dM}{dt} - \frac{dU}{dt} \right]. \quad (8)$$

In order to clarify the expressions of L_e and dU/dt , we denote $\tilde{U} = U - U_{\text{sh}}$, which represents the internal energy excluding the shock-accumulated part. The evolution of this internal energy component can be given by

$$\frac{d\tilde{U}}{dt} = \xi L_{\text{sd}} - \tilde{P} \frac{dV}{dt} - L_{\text{mn}}, \quad (9)$$

where $\tilde{P} = \tilde{U}/3V$ and

$$L_{\text{mn}} \approx \frac{\tilde{U}c}{r_{\text{m}}} \left[\frac{1 - e^{-(\tau_{\text{sh}} + \tau_{\text{un}})}}{\tau_{\text{sh}} + \tau_{\text{un}}} \right]. \quad (10)$$

This expression is different from Equation (6) because the majority of internal energy of the shocked region, which comes from the NS wind, is deposited in the most inner part of the region, which is much deeper than the shock front. Then we have $L_e = L_{\text{sh}} + L_{\text{mn}}$. The emission component represented by L_{mn} actually is the mergernova emission discussed in Yu et al. (2013).

¹For simplicity, in this paper we do not taken into account the relativistic effects that were considered in Yu et al. (2013) for some extremely light ejecta.

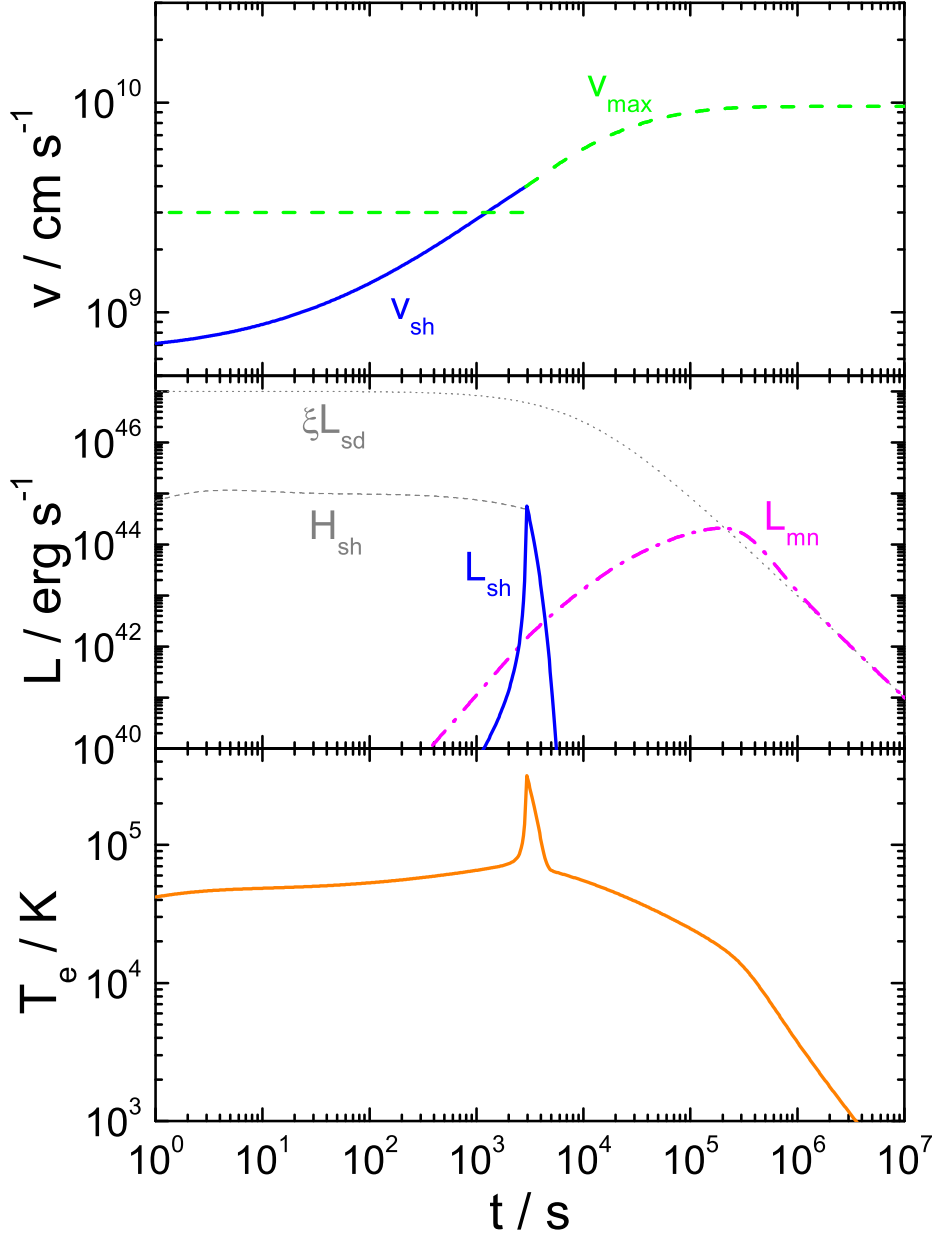


Fig. 1.— Evolutions of velocities (top), bolometric luminosities (middle), and emission temperature (bottom). In the middle panel, the injected spin-down luminosity (ξL_{sd}) and the shock heating rate (H_{sh}) are also presented for references. The model parameters are taken as $\xi L_{\text{sd},i} = 10^{47} \text{erg s}^{-1}$, $t_{\text{md}} = 10^4$ s, $\Delta t = 2$ s, $M_{\text{ej}} = 0.01 M_{\odot}$, $v_{\text{max}} = 0.1c$, $\delta = 3.5$, and $\kappa = 10 \text{cm}^2 \text{g}^{-1}$.

3. Results and analyses

A supra-massive NS surviving from a merger event is believed to initially spin with a Keplerian limit period of about 1 ms. This corresponds a rotational energy of several times 10^{52} erg with a high stellar mass, which could be much higher in view of the rapid differential rotation. The most of this energy is probably very quickly consumed to generate and amplify magnetic fields, to drive a short GRB, and maybe also to radiate GWs. The duration of this violent stage should not be much longer than the duration of the short GRB. So we would take $\Delta t = 2$ s which is the boundary dividing long and short GRBs. When a steady magnetic dipole radiation begins, the spin period could have been reduced to a few milliseconds, corresponding to an energy of $\sim 10^{51-52}$ erg. This energy supply could be further discounted for the merger ejecta by the parameter ξ , if a remarkable fraction is collimated within a small cone to power an extended gamma-ray emission and X-ray afterglow plateau after the GRB.

For typical values of spin-down luminosity and timescale as $\xi L_{\text{sd},i} = 10^{47} \text{erg s}^{-1}$ and $t_{\text{md}} = 10^4$ s, we present a representative numerical result in Figure 1. As shown in the top panel, the shock initially moves slowly, with a velocity much smaller than the maximum velocity of ejecta, and experiences a gradual acceleration process. When the shock velocity exceeds the maximum ejecta velocity by about a few tens percentage, shock breakout happens, as indicated by the sharp peak in the middle panel. It takes a remarkably long time ($\sim 10^3$ s) to break out from the ejecta by the shock. This period is much longer than the shock breakout time given in some previous works ($\sim 1 - 10$ s; Gao et al. 2013; Wang et al. 2015; Siegel & Ciolfi 2015a,b), where the shock acceleration process did not receive enough attention and then the shock velocity was significantly overestimated². The middle panel also shows the shock breakout emission is very luminous, which is comparable to that of the following bright mergernova emission peaking at a few days. Nevertheless, since the shock breakout and mergernova are emitted at very different radii, the corresponding emission temperature ($\sim 10^5$ K) of the former can be much higher than the latter ($\sim 10^4$ K), as presented in the bottom panel. Here an effective temperature is defined by $T_e = (L_e/4\pi r_{\text{max}}^2 \sigma)^{1/4}$ with σ being the Stefan-Boltzmann constant. In more details, we further plot three chromatic

²In these previous works, shock jump conditions were directly used to calculate the shock velocity, which is however inappropriate for a radiation-dominated shock. No matter which forms the NS wind is in, the energy injected into the ejecta should firstly be stored as internal energy. The ejecta can be accelerated only through the dissipation of this internal energy. Therefore, the shock jump conditions can be satisfied only after a long-term acceleration, before which the shock has crossed the whole ejecta.

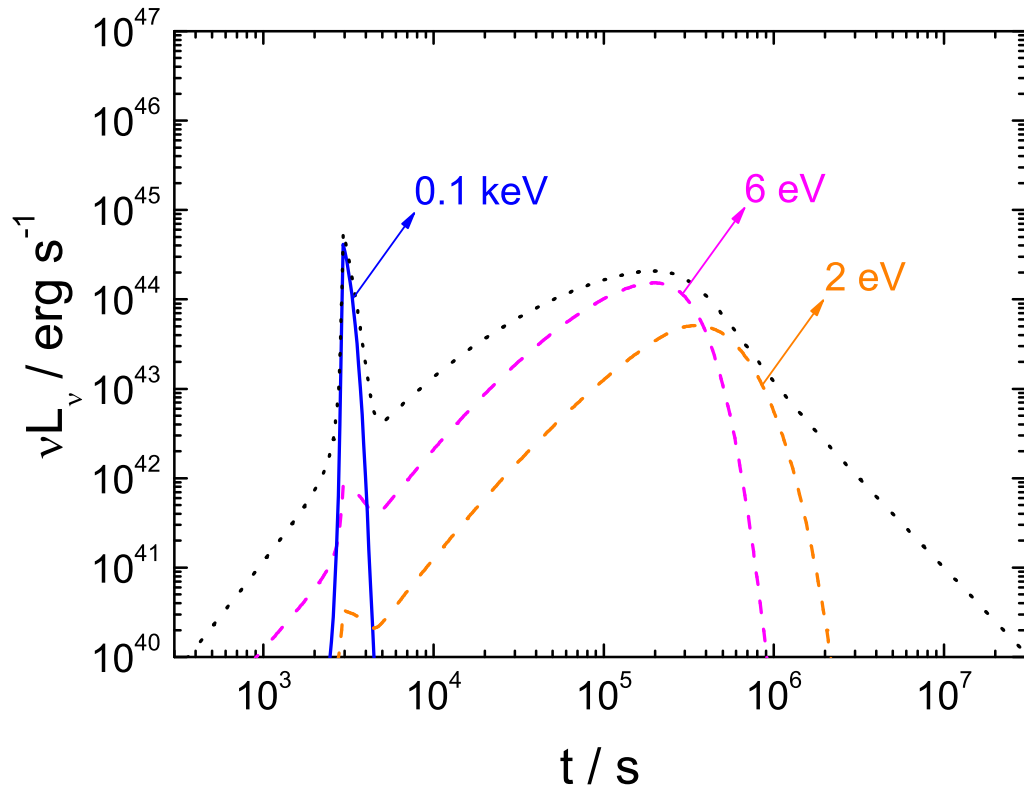


Fig. 2.— Three chromatic light curves for photon energies of $h\nu = 0.1$ keV (soft X-ray; solid), 6 eV (UV; dashed), and 2 eV (optical; dash-dotted), respectively, where the bolometric light curve (dotted) is presented for a reference.

light curves in Figure 2, by assuming a black-body spectrum³

$$\nu L_\nu = \frac{8\pi^2 r_{\max}^2}{h^3 c^2} \frac{(h\nu)^4}{\exp(h\nu/kT_e) - 1} \quad (11)$$

with temperatures given in the bottom panel of Figure 1, where h is the Planck constant and k the Boltzmann constant. As shown, while the mergernova emission falls into the ultraviolet band, the shock breakout is mainly concentrated within soft X-rays, for the adopted model parameters.

For a straightforward understanding of the characteristics of the shock breakout emission, here we provide some analytical analyses. Firstly, in physics, shock breakout happens when the dynamical time begins to be longer than the diffusion timescale on which photons diffuse from the shock front to the outmost surface of merger ejecta. Hence we can in principle solve the shock breakout time t_{bo} from the equation

$$\begin{aligned} t_{\text{bo}} = t_{\text{d}} &= \left(\frac{r_{\max} - r_{\text{sh,bo}}}{\lambda} \right)^2 \frac{\lambda}{c} \\ &= \frac{(r_{\max} - r_{\text{sh,bo}})^2 \kappa \rho_{\text{ej}}}{c}, \end{aligned} \quad (12)$$

where $\lambda = 1/(\kappa \rho_{\text{ej}})$ is the average path of photons. Approximately we get

$$r_{\text{sh,bo}} \approx r_{\max} \left(1 - \frac{r_{\max}}{r_*} \right), \quad (13)$$

where $r_* \approx (v_{\max} \kappa M_{\text{ej}}/c)^{1/2} = 4.5 \times 10^{15} \text{cm} (v_{\max}/0.1c)^{1/2} (\kappa/10 \text{cm}^2 \text{g}^{-1})^{1/2} (M_{\text{ej}}/0.01 M_\odot)^{1/2}$. This means, when the shock breakout happens, the shock radius has been very close to the maximum radius of ejecta. By invoking $U \sim \xi L_{\text{sd}} t$, $P = U/(3V)$, and acceleration rate $a \sim 4\pi r_{\text{sh}}^2 P/M$, we can estimate the breakout radius by $r_{\text{sh,bo}} \sim \frac{1}{2} a t_{\text{bo}}^2 \sim (\xi L_{\text{sd}}/2M_{\text{ej}})^{1/2} t_{\text{bo}}^{3/2}$, where $M \approx M_{\text{ej}}$ is adopted because $r_{\text{sh,bo}} \approx r_{\max}$. Then, from the equation $r_{\text{sh,bo}} \approx r_{\max} = v_{\max} t_{\text{bo}}$, we can simply derive the shock breakout time to

$$\begin{aligned} t_{\text{bo}} &\sim \frac{2M_{\text{ej}} v_{\max}^2}{\xi L_{\text{sd}}} \\ &= 3600 \text{s} \left(\frac{v_{\max}}{0.1c} \right)^2 \left(\frac{M_{\text{ej}}}{0.01 M_\odot} \right) \left(\frac{\xi L_{\text{sd}}}{10^{47} \text{erg s}^{-1}} \right)^{-1}. \end{aligned} \quad (14)$$

³In Yu et al. (2013), this spectrum is incorrectly written with an internal temperature rather than the effective surface temperature used here, although the integrated bolometric luminosity there is still right because of the reduction by optical depth.

Furthermore we get $v_{\text{sh,bo}} \sim 2v_{\text{max}}$ and $r_{\text{sh,bo}} \sim 2M_{\text{ej}}v_{\text{max}}^3/\xi L_{\text{sd}} = 1.1 \times 10^{13}\text{cm}$ that is indeed much smaller than r_* . Then the luminosity and temperature of shock breakout can be estimated to

$$\begin{aligned} L_{\text{sh,bo}} &\approx H_{\text{sh}} \sim 2\pi r_{\text{sh,bo}}^2 (v_{\text{sh,bo}} - v_{\text{max}})^3 \rho_{\text{ej}} \\ &\sim 8 \times 10^{45} \text{erg s}^{-1} \left(\frac{\xi L_{\text{sd}}}{10^{47} \text{erg s}^{-1}} \right), \end{aligned} \quad (15)$$

and

$$\begin{aligned} T_{\text{sh,bo}} &= \left(\frac{L_{\text{sh,bo}}}{4\pi r_{\text{max}}^2 \sigma} \right)^{1/4} \sim 6 \times 10^5 \text{K} \\ &\times \left(\frac{v_{\text{max}}}{0.1c} \right)^{-3/2} \left(\frac{M_{\text{ej}}}{0.01M_{\odot}} \right)^{-1/2} \left(\frac{\xi L_{\text{sd}}}{10^{47} \text{erg s}^{-1}} \right)^{3/4}. \end{aligned} \quad (16)$$

The above analytical expressions qualitatively exhibits the physical mechanisms and the parameter-dependencies of the shock breakout emission, although the numbers given here are somewhat higher than the numerical ones because a linear acceleration is assumed. In more details, in Figure 3 we present the variations of the shock breakout luminosity $L_{\text{sh,bo}}$ and the peak photon energy $\varepsilon_{\text{p}} = 4kT_{\text{sh,bo}}$ in the $\xi L_{\text{sd,i}} - t_{\text{md}}$ parameter space.

4. Conclusion and discussions

Mergernovae, in particular, the ones powered by a remnant supra-massive NS, are one of the most competitive electromagnetic counterparts of GW signals during NS-NS mergers. The discovery of NS-powered mergernovae could also substantially modify and expand our conventional understandings of supernova-like transient phenomena. Therefore, it would be an usual and essential question that how to identify a mergernova in future searchings and observations. Undoubtedly, a multi-wavelength method is necessary and helpful for answering this question. In this paper, we uncover that a shock breakout can be driven by the early interaction between a merger ejecta and a succeeding NS wind. Such a breakout appears at a few hours after the merger, by leading the mergernova emission as a precursor. The breakout emission would be mainly in soft X-rays with a luminosity of $\sim (10^{44} - 10^{46}) \text{erg s}^{-1}$, corresponding to an X-ray flux of a few $\times (10^{-11} - 10^{-9}) \text{erg s}^{-1}\text{cm}^{-2}$ for a distance of ~ 200 Mpc, which can be above the sensitivity of many current and future telescopes, e.g., Swift X-ray telescope (Burrows et al. 2005), Einstein Probe (Yuan et al. 2015), etc. More optimistically, some X-ray shock breakout emission could have been appeared in some X-ray afterglows of short GRBs, which probably exhibits as an early X-ray flare. It will be interesting to find out such candidates.

This work is supported by the National Basic Research Program of China (973 Program, grant 2014CB845800), the National Natural Science Foundation of China (grant No. 11473008), and the Program for New Century Excellent Talents in University (grant No. NCET-13-0822).

REFERENCES

- Abadie, J., Abbott, B. P., Abbott, R., et al. 2010, *CQGra*, 27, 173001
- Antoniadis, J., Freire, P. C. C., Wex, N., et al. 2013, *Science*, 340, 448
- Burrows, D. N., et al. 2005, *Space Sci. Rev.*, 120, 165
- Cheng, Q., & Yu, Y. W. 2014, *ApJ*, 786, L13
- Dessart, L., Ott, C. D., Burrows, A., et al. 2009, *ApJ*, 690, 1681
- Barnes, J., & Kasen, D. 2013, *ApJ*, 775, 18
- Bauswein, A., Goriely, S., & Janka, H. T. 2013a, *ApJ*, 773, 78
- Bauswein, A., Baumgarte, T. W., & Janka, H. T. 2013b, *Phys. Rev. Lett.*, 111, 131101
- Berger, E., Fong, W., & Chornock, R. 2013, *ApJ*, 774, L23
- Berger, E. 2014, *ARA&A*, 52, 43
- Dai, Z. G. 2004, *ApJ*, 606, 1000
- Dai, Z. G., Wang, X. Y., Wu, X. F., & Zhang, B. 2006, *Science*, 311, 1127
- Duncan, R. C., & Thompson, C. 1992, *ApJ*, 392, L9
- Fan, Y. Z., & Xu, D. 2006, *MNRAS*, 372, L19
- Fan, Y. Z., Yu, Y. W., Xu, D., et al. 2013, *ApJ*, 779, L25
- Fong, W., Berger, E., Metzger, B. D., et al. 2014, *ApJ*, 780, 118
- Gao, H., Ding, X., Wu, X. F., et al. 2013, *ApJ*, 771, 86
- Gao, H., Ding, X., Wu, X. F., et al. 2015, *ApJ*, 807, 163
- Giacomazzo, B., & Perna, R. 2013, *ApJ*, 771, L26

- Goriely, S., Bauswein, A., & Janka, H. T. 2011, *ApJ*, 738, L32
- Goriely, S. 2015, *The European Physical Journal A*, 51, 22
- Grossman, D., Korobkin, O., Rosswog, S., & Piran, T. 2014, *MNRAS*, 439, 757
- Hotokezaka, K., Kyutoku, K., Okawa, H., et al. 2011, *Phys. Rev. D*, 83, 124008
- Hotokezaka, K., Kiuchi, K., Kyutoku, K., et al. 2013, *Phys. Rev. D*, 87, 024001
- Hotokezaka, K., & Piran, T. 2015, *MNRAS*, 450, 1430
- Just, O., Bauswein, A., Pulpillo, R. A., et al. 2015, *MNRAS*, 448, 541
- Kasen, D., Badnell, N. R., & Barnes, J. 2013, *ApJ*, 774, 25
- Kasen, D., Fernández, R., & Metzger, B. D. 2015, *MNRAS*, 450, 1777
- Korobkin, O., Rosswog, S., Arcones, A., & Winteler, C. 2012, *MNRAS*, 426, 1940
- Kulkarni, S. R. 2005, arXiv: astro-ph/0510256
- Li, L. X., & Paczyński, B. 1998, *ApJ*, 507, L59
- Martin, D., Perego, A., Arcones, A., et al. 2015, arXiv:1506.05048
- Mao, Z., Yu, Y. W., Dai, Z. G., et al. 2010, *A&A*, 518, 27
- Metzger, B. D., Martinez-Pinedo, G., Darbha, S., et al. 2010, *MNRAS*, 406, 2650
- Metzger, B. D., & Berger, E. 2012, *ApJ*, 746, 48
- Metzger, B. D., & Fernández, R. 2014 *MNRAS*, 441, 3444
- Metzger, B. D., & Piro, A. L. 2014, *MNRAS*, 439, 3916
- Nakar, E. 2007, *PhR*, 442, 166
- Nakar, E., & Piran, T. 2011, *Nature*, 478, 82
- Nagakura, H., Hotokezaka, K., Sekiguchi, Y., et al. 2014, *ApJ*, 784, L28
- Nissanke, S., Holz, D. E., Dalal, N., et al. 2013, arXiv:1307.2638
- Oechslin, R., Janka, H. T., & Marek, A. 2007, *A&A*, 467, 395
- Perego, A., Rosswog, S., Cabezón, R. M., et al. 2014, *MNRAS*, 443, 3134

- Piran, T., Nakar, E., & Rosswog, S. 2013, MNRAS, 430, 2121
- Price, D. J., & Rosswog, S. 2006, Science, 312, 719
- Roberts, L. F., Kasen, D., Lee, W. H., et al. 2011, ApJ, 736, L21
- Rosswog, S., Liebendörfer, M., Thielemann, F. K., et al. 1999, A&A, 341, 499
- Rosswog, S. 2005 ApJ, 634, 1202
- Rosswog, S. 2013, Royal Society of London Philosophical Transactions Series A,, 371, 20120272
- Rosswog, S., Korobkin, O., Arcones, A., et al. 2014, MNRAS, 439, 744
- Rosswog, S. 2015, IJMPD, 24, 1530012
- Rowlinson, A., O’Brien, P. T., Tanvir, N. R., et al. 2010, MNRAS, 409, 531
- Rowlinson, A., O’Brien, P. T., Metzger, B. D., et al. 2013, MNRAS, 430, 1061
- Siegel, D. M., Ciolfi, R., & Rezzolla, L. 2014, ApJ, 785, L6
- Siegel, D. M., & Ciolfi, R. 2015, In Proceedings of Swift: 10 Years of Discovery, PoS(SWIFT 10)169(Trieste, Italy: Proceedings of Science, SISSA
- Siegel, D. M., & Ciolfi, R. 2015a, arXiv: 1508.07911
- Siegel, D. M., & Ciolfi, R. 2015b, arXiv: 1508.07939
- Tanaka, M., & Hotokezaka, K. 2013, ApJ, 775, 113
- Tanvir, N. R., Levan, A. J., Fruchter, A. S., et al. 2013, Nature, 500, 547
- van Eerten, H. J., & MacFadyen, A. I. 2012, ApJ, 747, L30
- Wanajo, S., Sekiguchi, Y., Nishimura, N., et al. 2014, ApJ, 789, L39
- Wang, L. J., Dai, Z. G., & Yu, Y. W. 2015, ApJ, 800, 79
- Yu, Y. W., Cheng, K. S., & Cao, X. F. 2010, ApJ, 715, 477
- Yu, Y. W., Zhang, B., & Gao, H. 2013, ApJ, 776, L40
- Yu, Y. W., Li, S. Z., & Dai, Z. G. 2015, ApJ, 806, L6
- Yuan, W., Zhang, C., Feng, H. et al., 2015, arXiv:1506.07735

Zhang, B., & Yan, H. R. 2011, ApJ, 726, 90

Zhang, B. 2013, ApJ, 763, L22

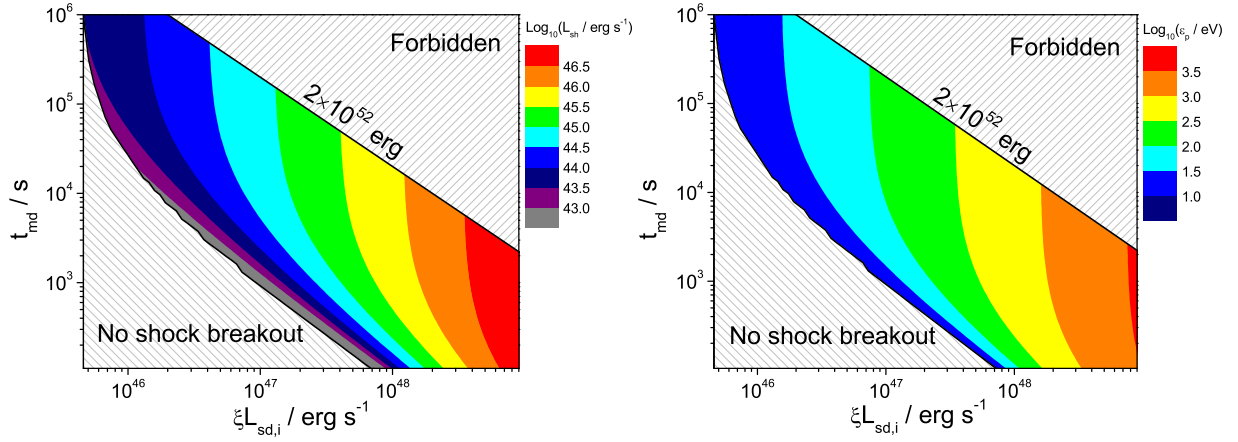


Fig. 3.— Variations of the luminosity (left) and peak photon energy (right) of shock breakout emission in the $\xi L_{\text{sd},i} - t_{\text{md}}$ parameter space. The shaded region on the right-top corner is forbidden because an unrealistically high rotational energy is required, while in the left-bottom shaded region the shock breakout is buried in the mergernova emission.